



A prospective head-to-head comparison of [^{68}Ga]Ga-P16-093 and [^{68}Ga]Ga-PSMA-11 PET/CT in patients with primary prostate cancer

Guochang Wang¹ · Linlin Li¹ · Ming Zhu² · Jie Zang³ · Jiarou Wang¹ · Rongxi Wang¹ · Weigang Yan² · Lin Zhu⁴ · Hank F. Kung⁵ · Zhaohui Zhu¹

Received: 3 April 2023 / Accepted: 19 May 2023

© The Author(s), under exclusive licence to Springer-Verlag GmbH Germany, part of Springer Nature 2023

Abstract

Purpose We aimed to compare the diagnostic performance and biodistribution of two similar PET agents, [^{68}Ga]Ga-P16-093 and [^{68}Ga]Ga-PSMA-11, in the same group of primary prostate cancer (PCa) patients.

Methods Fifty patients with untreated, histologically confirmed PCa by needle biopsy were enrolled. Each patient underwent [^{68}Ga]Ga-P16-093 and [^{68}Ga]Ga-PSMA-11 PET/CT within a week. In addition to visual analysis, the standardized uptake value (SUV) was measured for semiquantitative comparison and correlation analysis.

Results [^{68}Ga]Ga-P16-093 PET/CT detected more positive tumors than [^{68}Ga]Ga-PSMA-11 PET/CT (202 vs. 190, $P=0.002$), both for intraprostatic lesions (48 vs. 41, $P=0.016$) and metastatic lesions (154 vs. 149, $P=0.125$), especially for intraprostatic lesions in low- and intermediate-risk PCa patients (21/23 vs. 15/23, $P=0.031$). Furthermore, [^{68}Ga]Ga-P16-093 PET/CT exhibited a significantly higher SUVmax for most matched tumors (13.7 ± 10.2 vs. 11.4 ± 8.3 , $P<0.001$). For normal organs, [^{68}Ga]Ga-P16-093 PET/CT showed significantly lower activity in the kidney (SUVmean: 20.1 ± 6.1 vs. 29.3 ± 9.1 , $P<0.001$) and urinary bladder (SUVmean: 6.5 ± 7.1 vs. 20.9 ± 17.4 , $P<0.001$), but displayed a higher uptake in the parotid gland (SUVmean: 8.7 ± 2.6 vs. 7.6 ± 2.1 , $P<0.001$), liver (SUVmean: 7.0 ± 1.9 vs. 3.7 ± 1.3 , $P<0.001$), and spleen (SUVmean: 8.2 ± 3.0 vs. 5.2 ± 2.2 , $P<0.001$) than [^{68}Ga]Ga-PSMA-11 PET/CT.

Conclusion [^{68}Ga]Ga-P16-093 PET/CT demonstrated higher tumor uptake and better tumor detectability than [^{68}Ga]Ga-PSMA-11 PET/CT, especially in low- and intermediate-risk PCa patients, which indicated that [^{68}Ga]Ga-P16-093 may serve as an alternative agent for detection of PCa.

Trial registration ^{68}Ga -P16-093 and ^{68}Ga -PSMA-11 PET/CT Imaging in the Same Group of Primary Prostate Cancer Patients (NCT05324332, Registered 12 April 2022, retrospectively registered).

URL of registry <https://clinicaltrials.gov/ct2/show/NCT05324332>.

Keywords [^{68}Ga]Ga-P16-093 · [^{68}Ga]Ga-PSMA-11 · Prostate cancer · PET/CT

Introduction

Prostate-specific membrane antigen (PSMA) is an ideal target for accurate diagnosis and therapy in prostate cancer (PCa), as it is overexpressed in prostatic carcinoma cells [1], and multiple PSMA-targeted radiopharmaceuticals have been developed and introduced in this field. [^{68}Ga]Ga-PSMA-11 (also known as [^{68}Ga]Ga-HBED-CC-PSMA,

approved by FDA in 2020 [2], and its new kit formulation LOCAMETZ approved in 2022 [3]) was the first commonly applied imaging agent in staging and restaging of PCa and evaluating the therapeutic effect. Other radiotracers, such as [^{18}F]DCFPyL (PYLARIFY®, piflufolastat F 18, approved by FDA in 2021), [^{68}Ga]Ga-PSMA-I&T, [^{18}F]F-PSMA-1007 and many other related derivatives, are also widely used in clinical research [4–7]. However, some literatures suggested that the high urinary excretion of [^{68}Ga]Ga-PSMA-11, especially when there was intense urinary bladder activity, may impede the identification of small volume diseases close to the bladder, ureters, and prostatic urethra [8, 9].

Guochang Wang, Linlin Li, and Ming Zhu contributed equally to this work.

Extended author information available on the last page of the article

We synthesized a new PSMA-targeted radiopharmaceutical, named [^{68}Ga] Ga -P16-093, which targets cellular PSMA using the urea fragment of a conjugate that employs the HBED-CC chelator for labelling with [^{68}Ga](III). [^{68}Ga] Ga -P16-093 is a close analog of [^{68}Ga] Ga -PSMA-11, and the *O*-(carboxymethyl)-*L*-tyrosine linker provides [^{68}Ga] Ga -P16-093 with optimal PSMA binding affinity and superior in vivo pharmacokinetics [10, 11]. Previously, a preliminary comparison study enrolled 10 PCa patients with biochemical recurrence for head-to-head comparison in the same patient. Results showed that [^{68}Ga] Ga -P16-093 was cleared rapidly from the blood. When measuring radioactivity in the urinary bladder, [^{68}Ga] Ga -P16-093 demonstrated a measurable reduction compared to [^{68}Ga] Ga -PSMA-11 in a similar time period; therefore, it may be advantageous in the detection of lesions near the urinary bladder because of less interference [12]. Another study measured the accuracy of PSMA-PET based on [^{68}Ga] Ga -P16-093 or [^{68}Ga] Ga -PSMA-11 in evaluating nerve bundle invasion and compared it with standard-of-care predictors including MRI and biopsy, which confirmed presurgical PSMA-PET imaging can improve surgical guidance in men with Gleason $\geq 4+3$ prostate cancer resulting in preservation of nerve-bundles [13]. Other head-to-head studies compared the early kinetics and diagnostic performance between [^{68}Ga] Ga -P16-093 and [^{68}Ga] Ga -PSMA-617 positron emission tomography/computed tomography (PET/CT) in a group of PCa patients, which revealed higher tumor uptake, tumor-to-blood pool ratio, detection capability and less blood pool and bladder accumulation when using [^{68}Ga] Ga -P16-093 PET/CT [14, 15].

This head-to-head study aimed to further evaluate the diagnostic performance and physiological distribution of [^{68}Ga] Ga -P16-093 against [^{68}Ga] Ga -PSMA-11 in a group of treatment-naïve primary PCa patients.

Materials and methods

This study was approved by the Institutional Review Board of Peking Union Medical College Hospital (no. ZS-2461) and was registered at clinicaltrials.gov (NCT05324332). From April 2022 to October 2022, 50 patients with newly diagnosed, histologically confirmed PCa by needle biopsy were recruited into the cohort. Patients who had accepted any form of therapy against PCa before PET scan were excluded from the study. The initial risk stratification of PCa was confirmed based on the D'Amico classification [16]. Written informed consent was obtained from each patient prior to this study.

Synthesis of radiopharmaceuticals

The radiolabelling of [^{68}Ga] Ga -P16-093 was performed as described previously. Briefly, [^{68}Ga] GaCl_3 was eluted from a Ge-68/ Ga -68 generator produced by Eckert & Ziegler using 5 mL of 0.1 M ultrapure hydrochloride acid, 2 mL eluted [^{68}Ga] GaCl_3 solution was added to a reaction vial, which contained P16-093 (15 μg) and $\text{NaOAc}\cdot 3\text{H}_2\text{O}$ (68 mg) as a lyophilized powder. The reaction mixture was heated for 5 min at 95°C. Subsequently, the final product was diluted with saline and sterilized by filtered through a 0.2- μm sterile vented PVDF filter into a sterile septum-capped vial [14].

[^{68}Ga] Ga -PSMA-11 was prepared manually using a kit containing 12 μg of PSMA-11 as the precursor and 40 mg of NaOAc at room temperature, and the process of labelling with Ga -68 was the same for [^{68}Ga] Ga -P16-093.

The quality control of the labelled radiotracers was analyzed by iTLC assessment. The radiochemical purities of the two imaging agents were over 95%.

PET/CT imaging acquisition

[^{68}Ga] Ga -P16-093 and [^{68}Ga] Ga -PSMA-11 PET/CT scans in each patient were conducted on different days within 1 week using a dedicated PET/CT scanner (Biograph 64 TruePoint TrueV [Siemens]). The patients were instructed to drink approximately 500 mL of water within 1–2 h and to void immediately before the PET scan. PET/CT images were obtained 50–60 min after an intravenous injection of either [^{68}Ga] Ga -P16-093 or [^{68}Ga] Ga -PSMA-11 at a dosage of 1.8–2.2 MBq (0.05–0.06 mCi)/kg [17]. All patients started with a low-dose CT (120 keV; 50 mAs; 1.3 pitch; 2.5 mm slice thickness; 0.5 s rotation time; estimated radiation dose, 9.0 mGy) for attenuation correction and anatomical localization from the skull vertex to the proximal thigh, followed by a PET scan at 2 min/bed position. The acquired data were reconstructed using ordered-subset expectation maximization (Siemens Biograph 64: 2 iterations, 8 subsets, Gaussian filter of 5 mm in full width at half maximum, 168 \times 168 image size).

Imaging analysis

All images were transferred to MIM software (Version 7.1.4, MIM Software Inc., Cleveland, USA) and were interpreted independently by two experienced nuclear medicine physicians who were blinded to the clinical history of the patients, and any disagreement was resolved by consensus. The maximum standardized uptake value (SUVmax) calculation in the tumor was based on body weight and was calculated using a spherical volume of interest (VOI) that sufficiently

covered the lesion. Any focal tracer accumulation above the surrounding background activity that could not be explained by the physiological tracer uptake was interpreted as a tumor [18, 19]. Typical pitfalls in PSMA PET/CT were also considered [20]. The mean standardized uptake value (SUVmean) of selected normal tissues was established on the right side of the parotid gland, blood pool (arcus aortae level), liver, spleen, left kidney, duodenum (horizontal part), gluteal musculature, normal prostate, and urinary bladder; organ-gluteal uptake ratio was measured by dividing the SUVmean of normal tissues by the SUVmean of the background (gluteal musculature).

Immunohistochemistry

PSMA expression in intraprostatic tumor was examined using obtainable biopsy samples via immunohistochemistry performed according to previously described protocol [21]. The immunohistochemical results were assessed as a visualized percentage of positively staining cells and grade of color intensity (staining) following the immunoreactive score (IRS) and reported with a 4-point IRS classification [21, 22].

Statistical analysis

All statistical analyses were conducted using SPSS software (Version 26.0, IBM Corp, Armonk, NY, USA) and GraphPad Prism (Version 9.4.1, GraphPad Software, San Diego, CA, USA). The quantitative data are presented as the mean \pm standard deviation. The McNemar test and Wilcoxon signed-rank test were used to compare the detection rates of [^{68}Ga]Ga-P16-093 and [^{68}Ga]Ga-PSMA-11 PET/CT. The differences in tumor uptake and normal organ activity between [^{68}Ga]Ga-P16-093 and [^{68}Ga]Ga-PSMA-11 were evaluated using paired *t* tests. The cutoff, sensitivity, and specificity of SUVmax were calculated based on receiver operating characteristic (ROC) curves. The area under the ROC curve (AUC) was presented with 95% confidence intervals (CI), and the differences between AUC (ΔAUC) and *P* values were calculated using DeLong's test. Spearman correlation coefficient was used for correlation analysis. A *P* value <0.05 was considered statistically significant.

Results

Characteristics of enrolled patients

The average age of the 50 men enrolled in the study was 67.7 ± 6.4 years (range 49–81 years, median 68 years), with a mean biopsy Gleason Score of 7.7 ± 1.3 (range 6–10, median 7) and a mean serum PSA level of

79.6 ± 120.3 ng/mL (range 3.9–595.0 ng/mL, median 17.4 ng/mL). The median interval between prostate biopsy and PET imaging was 17 days (range 14–22 days). Due to COVID-19 restrictions, not all PCa patients were returned for scheduled surgery; therefore, collections of surgical pathological samples were limited, whereas we obtained prostate biopsy pathologies in all enrolled patients. Further patient characteristics are summarized in Table 1. No adverse events were observed in any patient after the administration of the radiopharmaceuticals.

Biodistribution comparison between [^{68}Ga]Ga-P16-093 and [^{68}Ga]Ga-PSMA-11

In general, [^{68}Ga]Ga-P16-093 PET/CT showed a lower urinary background and higher hepatobiliary excretion than [^{68}Ga]Ga-PSMA-11 PET/CT, demonstrating in the kidney (SUVmean: 20.1 ± 6.1 vs. 29.3 ± 9.1 , $P < 0.001$), bladder (SUVmean: 6.5 ± 7.1 vs. 20.9 ± 17.4 , $P < 0.001$), liver (SUVmean: 7.0 ± 1.9 vs. 3.7 ± 1.3 , $P < 0.001$), and spleen (SUVmean: 8.2 ± 3.0 vs. 5.2 ± 2.2 , $P < 0.001$). The average SUVmean of all measured normal organs and organ-gluteal uptake ratio on [^{68}Ga]Ga-P16-093 and [^{68}Ga]Ga-PSMA-11 PET/CT is shown in Table 2.

Table 1 Patient characteristics

Characteristic	Summary
Number of patients	50
Age in years, median (range)	68 (49–81)
PSA ng/ml, median (range)	17.4 (3.9–595.0)
Clinical Stage	
cT1- cT2a	11 (22.0%)
cT2b-cT2c	17 (34.0%)
\geq T3a	22 (44.0%)
Biopsy Gleason Score	
6	9 (18.0%)
7 ^a	7 (14.0%)
7 ^{a,b}	10 (20.0%)
8	10 (20.0%)
9	8 (16.0%)
10	6 (12.0%)
D'Amico classification	
Low risk	7 (14.0%)
Intermediate risk	16 (32.0%)
High risk	27 (54.0%)
Metastasis	
None	35 (70.0%)
Lymph node metastasis	7 (14.0%)
Bone metastasis	11 (22.0%)

^a Predominant Gleason score 3; ^b Predominant Gleason score 4

Table 2 The average SUVmean of all measured normal organs and organ-gluteal uptake ratio on [^{68}Ga]Ga-P16-093 and [^{68}Ga]Ga-PSMA-11 PET/CT

Normal organ	Organ uptake (SUVmean)			Organ-gluteal uptake ratio		
	[^{68}Ga]Ga-P16-093	[^{68}Ga]Ga-PSMA-11	<i>P</i> value	[^{68}Ga]Ga-P16-093	[^{68}Ga]Ga-PSMA-11	<i>P</i> value
Parotid gland	8.7 ± 2.6	7.6 ± 2.1	< 0.001*	19.5 ± 8.2	17.6 ± 6.7	0.001*
Blood pool	1.2 ± 0.3	1.2 ± 0.7	0.610	2.6 ± 0.7	2.7 ± 0.9	0.813
Liver	7.0 ± 1.9	3.7 ± 1.3	< 0.001*	15.9 ± 6.0	8.7 ± 3.7	< 0.001*
Spleen	8.2 ± 3.0	5.2 ± 2.2	< 0.001*	18.4 ± 8.6	11.9 ± 5.0	< 0.001*
Duodenum	7.8 ± 2.7	7.3 ± 2.3	0.171	17.1 ± 6.3	17.1 ± 6.1	0.088
Kidney	20.1 ± 6.1	29.3 ± 9.1	< 0.001*	44.4 ± 16.5	66.3 ± 25.1	< 0.001*
Bladder	6.5 ± 7.1	20.9 ± 17.4	< 0.001*	13.3 ± 16.0	50.3 ± 46.6	< 0.001*
Prostate	1.2 ± 0.3	1.3 ± 0.3	0.429	6.1 ± 2.3	6.3 ± 2.0	0.043*
Gluteal musculature	0.5 ± 0.2	0.5 ± 0.2	0.248	-	-	-

* The difference was statistically significant

Tumor detection capability

Among the 50 primary PCa patients, [^{68}Ga]Ga-P16-093 PET/CT detected 202 lesions in 48 (96.0%) patients, and [^{68}Ga]Ga-PSMA-11 identified 190 tumors in 41 (82.0%) patients. [^{68}Ga]Ga-P16-093 PET/CT demonstrated a significantly higher detection rate than [^{68}Ga]Ga-PSMA-11 PET/CT (per-patient analysis, $P = 0.016$; per-lesion analysis, $P = 0.002$).

For the intraprostatic tumors, [^{68}Ga]Ga-P16-093 PET/CT identified 48 PSMA-avid lesions, [^{68}Ga]Ga-PSMA-11 PET/CT visually detected 41 primary tumors ($P = 0.016$), [^{68}Ga]Ga-P16-093 PET/CT detected 7 additional intraprostatic lesions than [^{68}Ga]Ga-PSMA-11 PET/CT, as shown in Fig. 1, and there were no intraprostatic tumors that showed negative [^{68}Ga]Ga-P16-093 uptake but positive [^{68}Ga]Ga-PSMA-11 uptake; whereas 2 primary lesions were missed by both PET scans. To be more exact, in the low- and intermediate-risk PCa patients, [^{68}Ga]Ga-P16-093 PET/CT demonstrated significantly better tumor detectability than [^{68}Ga]Ga-PSMA-11 PET/CT (21/23 vs. 15/23, $P = 0.031$), whereas the detection rates of the two scans showed no statistically significant difference in the high-risk patients (27/27 vs. 26/27, $P = 1.000$). For metastatic tumors, [^{68}Ga]Ga-P16-093 PET/CT revealed 154 PSMA-positive lesions, and [^{68}Ga]Ga-PSMA-11 PET/CT depicted 149 PSMA-avid lesions ($P = 0.125$), as shown in Fig. 2. The detailed diagnostic performances of [^{68}Ga]Ga-P16-093 and [^{68}Ga]Ga-PSMA-11 PET/CT for the primary PCa patients is shown in Table 3.

Comparison of tumor uptake

For matched tumors, there was a strong positive correlation between the two tracer uptakes of [^{68}Ga]Ga-P16-093 and [^{68}Ga]Ga-PSMA-617 ($r = 0.938$, $P < 0.001$). [^{68}Ga]Ga-P16-093 PET/CT revealed significantly higher tumor uptake on

almost all the matched tumors in comparison to [^{68}Ga]Ga-PSMA-11 PET/CT (13.7 ± 10.2 vs. 11.4 ± 8.3 , $P < 0.001$). The detailed tumor uptake of [^{68}Ga]Ga-P16-093 and [^{68}Ga]Ga-PSMA-11 PET/CT for the primary PCa patients is shown in Table 3.

The AUCs (sensitivity/specificity) of the intraprostatic tumors for [^{68}Ga]Ga-P16-093 and [^{68}Ga]Ga-PSMA-11 PET/CT were 0.991 (95% CI: 0.939–1.000) and 0.906 (95% CI: 0.822–0.959), respectively. The ΔAUC between the two imaging modalities was statistically significant ($P = 0.007$). The cutoff SUVmax of [^{68}Ga]Ga-P16-093 and [^{68}Ga]Ga-PSMA-11 PET/CT were 3.9 (sensitivity, 0.939; specificity, 0.941) and 4.1 (sensitivity, 0.735; specificity, 0.941), respectively. The SUVmax of the intraprostatic tumors on [^{68}Ga]Ga-P16-093 and [^{68}Ga]Ga-PSMA-11 PET/CT were moderately correlated with the biopsy Gleason Score (for [^{68}Ga]Ga-P16-093: $r = 0.488$, $P = 0.003$; for [^{68}Ga]Ga-PSMA-11: $r = 0.509$, $P = 0.001$) and serum PSA value (for [^{68}Ga]Ga-P16-093: $r = 0.505$, $P < 0.001$; for [^{68}Ga]Ga-PSMA-11: $r = 0.457$, $P = 0.001$), respectively. On patient-based analysis, the high-risk PCa patients exhibited a higher SUVmax on PSMA PET/CT for the prostatic tumors than the low- and intermediate-risk PCa patients (for [^{68}Ga]Ga-P16-093: 19.6 ± 16.1 vs. 6.8 ± 2.4 vs. 11.0 ± 9.2 , $P = 0.023$; for [^{68}Ga]Ga-PSMA-11: 15.8 ± 10.6 vs. 4.1 ± 0.7 vs. 9.6 ± 2.1 , $P = 0.011$), as shown in Fig. 3.

PSMA immunohistochemical staining

Thirty-seven biopsy samples of intraprostatic tumors were analyzed with the immunohistochemical stain of PSMA expression, the other 13 samples could not be analyzed for immunohistochemical stain because the tissue volume was too small. The PSMA expression of the primary tumor was weak in 3, moderate in 11, and strong in 23 cases. The SUVmax as measured by [^{68}Ga]Ga-P16-093 and [^{68}Ga]Ga-

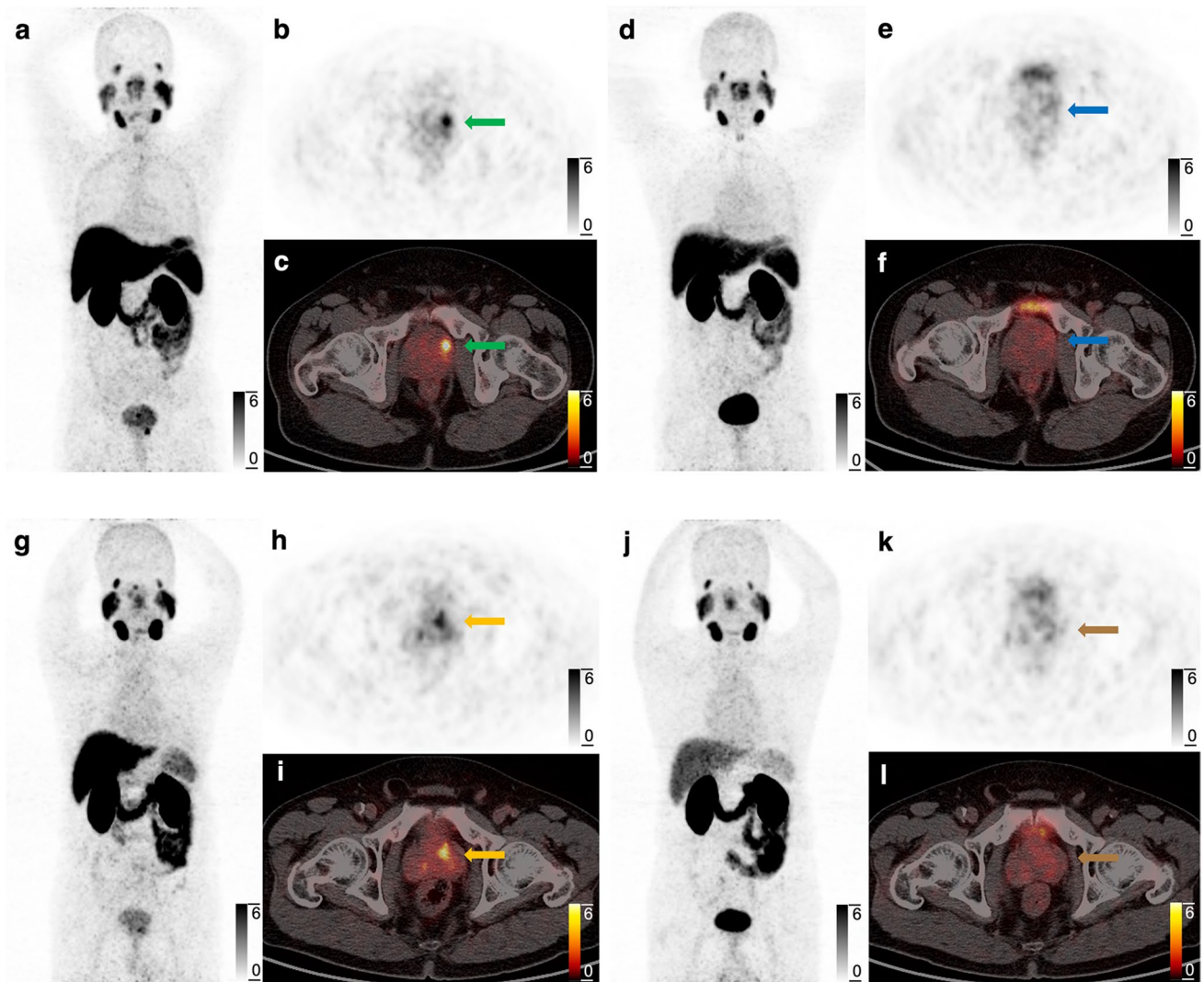


Fig. 1 Performance of [^{68}Ga]Ga-P16-093 and [^{68}Ga]Ga-PSMA-11 PET/CT in two patients with primary prostate cancer. (First row) A 68-year-old male with a Gleason Score of 3+4 and a PSA level of 16.8 ng/mL. [^{68}Ga]Ga-P16-093 PET/CT (a-c) revealed a PSMA-avid tumor in the prostate (green arrow, SUVmax 7.5), which was negative on [^{68}Ga]Ga-PSMA-11 PET/CT (d-f, blue arrow). (Second row)

A 67-year-old male with a Gleason Score of 3+3 and a PSA level of 7.9 ng/mL. [^{68}Ga]Ga-P16-093 PET/CT (g-i) depicted increased tracer uptake in the intraprostatic tumor (orange arrow, SUVmax 5.1), and [^{68}Ga]Ga-PSMA-11 PET/CT (j-l) exhibited unremarkable uptake (brown arrow)

Ga-PSMA-11 PET/CT showed significant associations with PSMA IRS (for [^{68}Ga]Ga-P16-093: $r=0.786$, $P<0.001$; for [^{68}Ga]Ga-PSMA-11: $r=0.815$, $P<0.001$), as shown in Fig. 4.

Discussion

This is a prospective head-to-head comparison of [^{68}Ga]Ga-P16-093 and [^{68}Ga]Ga-PSMA-11 PET/CT in a group of primary PCa patients. Results showed that [^{68}Ga]Ga-P16-093 PET/CT exhibited significantly better detection rate and higher tumor uptake than [^{68}Ga]Ga-PSMA-11 PET/CT.

Over the past decade, the usefulness of [^{68}Ga]Ga-PSMA-11 PET/CT for staging and restaging in PCa has been well recognized [19, 23, 24]. However, Zhou et al. reported that [^{68}Ga]Ga-PSMA-11 PET/CT revealed a relatively poor detection rate of intraprostatic tumors in low- and intermediate-risk PCa patients compared with high-risk patients, and the detection rates were 21/35 (60.0%) and 64/66 (97.0%), respectively [25]. In another report, Uprimny et al. concluded that [^{68}Ga]Ga-PSMA-11 PET/CT should only be preferentially applied for the primary staging of PCa in patients with a Gleason Score >7 or a PSA level ≥ 10 ng/ml due to the low [^{68}Ga]Ga-PSMA-11 uptake in low-risk PCa patients [20]. At present, clinical studies

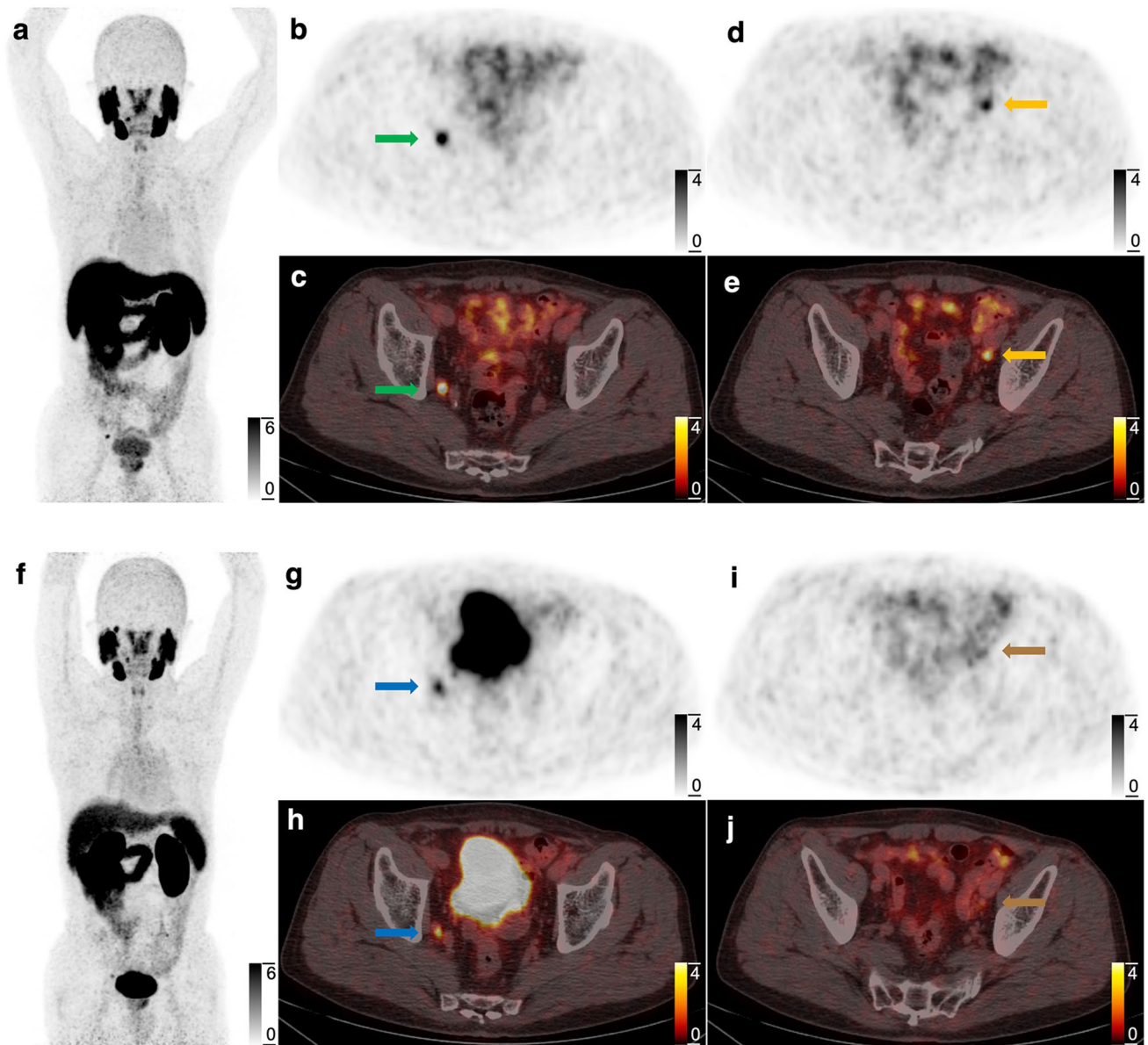


Fig. 2 A 77-year-old primary prostate cancer patient with a Gleason score of 4+4 and a PSA level of 62.9 ng/mL. Anterior MIP image as well as axial [^{68}Ga]Ga-P16-093 PET/CT (a-e) show distinct tracer uptakes in two lymph nodes beside the bilateral iliac vessels (green arrow, SUVmax 5.9; orange arrow, SUVmax 3.8); however, only the

right para-iliac lymph node was identifiable on [^{68}Ga]Ga-PSMA-11 PET/CT (f-h, blue arrow, SUVmax 3.7). The lesion beside the left iliac vessel revealed unnoticed uptake (brown arrow, SUVmax 2.5). Subsequently, lymphadenectomy confirmed bilateral metastatic prostate cancers

of [^{68}Ga]Ga-PSMA-11 for the initial staging in low- and intermediate-risk PCa patients are relatively rare and thus may be insufficient to draw a generalized, clear conclusion that [^{68}Ga]Ga-PSMA-11 PET/CT is less efficient in diagnosing low-risk PCa. In our study, [^{68}Ga]Ga-P16-093 PET/CT demonstrated better detection efficiency and sensitivity of intraprostatic tumors in low- and intermediate-risk PCa than [^{68}Ga]Ga-PSMA-11 PET/CT, which may benefit more patients. In addition, [^{68}Ga]Ga-P16-093 PET/CT also detected a small amount extra lymph node metastases and

bone metastases in comparison to [^{68}Ga]Ga-PSMA-11 PET/CT. In most cases, however, these findings did not alter the overall staging of the disease because there were already additional detected sites of either nodal or bone metastases. Even so, this information may still play a crucial role in the choice of treatment modality, in the preoperative surgical planning, and for guiding the extent of radiotherapy treatment [7]. All these findings suggest that [^{68}Ga]Ga-P16-093 may be a promising novel radiotracer for diagnosis and initial staging in PCa patients.

Table 3 Detectability and tumor uptake of [^{68}Ga]Ga-P16-093 and [^{68}Ga]Ga-PSMA-11 PET/CT in primary PCa patients

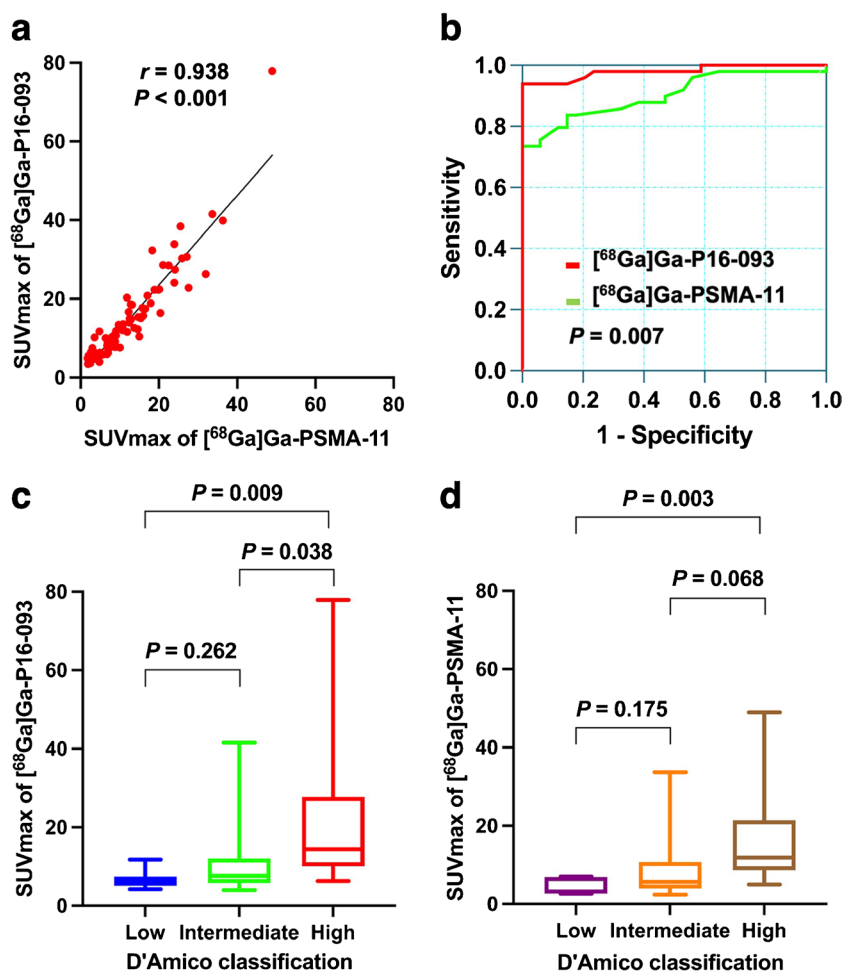
Involvement of tumor	Tumor detectability			Tumor uptake (SUVmax)		
	[^{68}Ga]Ga-P16-093	[^{68}Ga]Ga-PSMA-11	<i>P</i> value	[^{68}Ga]Ga-P16-093	[^{68}Ga]Ga-PSMA-11	<i>P</i> value
Intraprostatic tumors	48	41	0.016*	14.5 ± 13.4	11.6 ± 10.1	0.001*
Low- and Intermediate-risk group	21	15	0.031*	10.1 ± 8.6	7.8 ± 7.5	< 0.001*
High-risk group	27	26	1.000	19.6 ± 16.1	15.8 ± 10.6	0.002*
Metastatic tumors	154	149	0.125	13.3 ± 8.4	11.3 ± 7.5	< 0.001*
Lymph node metastases	24	21	0.625	15.4 ± 10.3	13.2 ± 8.0	< 0.001*
Bone metastases	130	128	0.443	11.7 ± 6.1	9.8 ± 5.6	< 0.001*
Total lesions	202	190	0.002*	13.7 ± 10.2	11.4 ± 8.3	< 0.001*

* The difference was statistically significant

[^{68}Ga]Ga-P16-093 PET/CT showed a significantly higher uptake in almost all tumors than [^{68}Ga]Ga-PSMA-11 PET/CT, which may not be of particular significance or useful in high-risk patients but may be a critical factor for improving the tumor detection rate in low- and intermediate-risk patients. The tumor uptakes based on [^{68}Ga]Ga-P16-093 and [^{68}Ga]Ga-PSMA-11 PET/CT reported in this paper

were correlated with the biopsy Gleason scores, serum PSA values as well as with the PSMA IRS. These results are considerably consistent with other previous studies [15, 26, 27]. Furthermore, in this study, the tumor uptake of [^{68}Ga]Ga-P16-093 in the high-risk PCa group was consistently higher than that of the tumors in the low- and intermediate-risk PCa groups. More studies are needed to confirm

Fig. 3 Significant correlation between the SUVmax on [^{68}Ga]Ga-P16-093 and [^{68}Ga]Ga-PSMA-11 PET/CT (a); ROC curves for [^{68}Ga]Ga-P16-093 and [^{68}Ga]Ga-PSMA-11 PET/CT (b); significantly higher tumor SUVmax for high-risk PCa patients than for low- and intermediate-risk PCa patients on [^{68}Ga]Ga-P16-093 PET/CT (c) and [^{68}Ga]Ga-PSMA-11 PET/CT (d)



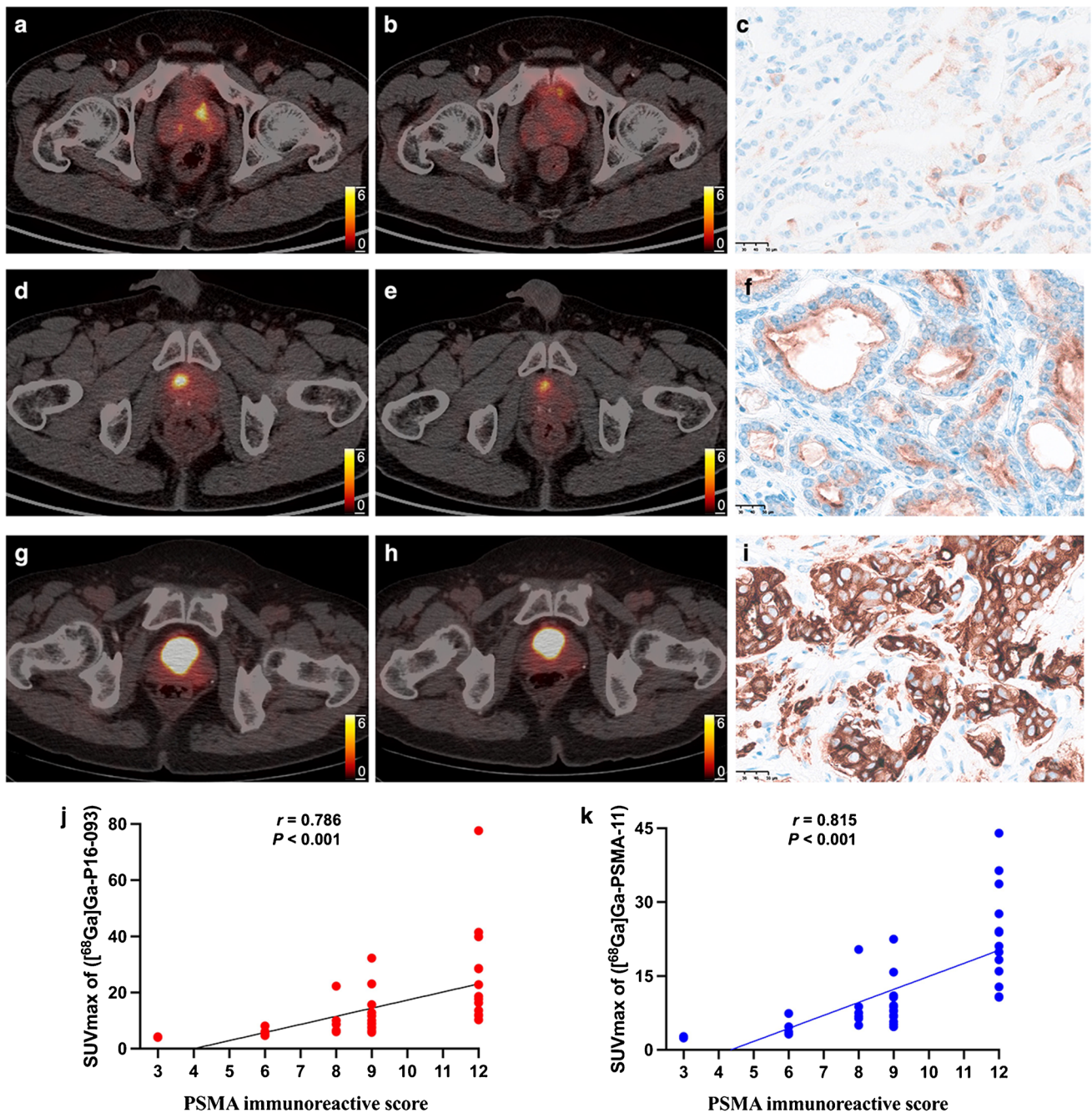


Fig. 4 PSMA-immunohistochemistry of three typical cases of prostate cancer. The **a**, **d**, **g** represented fusion images of three patients based on $[^{68}\text{Ga}]\text{Ga-P16-093}$ PET/CT; **b**, **e**, **h** represented fusion images of three patients based on $[^{68}\text{Ga}]\text{Ga-PSMA-11}$ PET/CT; **c**, **f**, **i** represented weak, moderate, and strong PSMA expression, respectively. Significantly correlation between the SUVmax on $[^{68}\text{Ga}]\text{Ga-P16-093}$, $[^{68}\text{Ga}]\text{Ga-PSMA-11}$ PET/CT and PSMA immunoreactive score (**j**, **k**)

whether uptake level of intraprostatic tumor by $[^{68}\text{Ga}]\text{Ga-P16-093}$ PET/CT could be used an alternative risk grading marker of PCa.

Regarding the physiological distribution of both tracers, $[^{68}\text{Ga}]\text{Ga-P16-093}$ displayed a significantly lower urinary excretion. More precisely, the kidney and bladder retention rates of $[^{68}\text{Ga}]\text{Ga-P16-093}$ were 31.4% and 68.9% lower

than those of $[^{68}\text{Ga}]\text{Ga-PSMA-11}$, which was similar to $[^{18}\text{F}]\text{F-PSMA-1007}$ [28]. The slower renal excretion rate of $[^{68}\text{Ga}]\text{Ga-P16-093}$ may enable a more accurate interpretation of tumor location that may be impacted by the urine retention inside the bladder [28]. This may also allow the avoidance of diuretic administration and time-consuming delayed imaging acquisition. Besides, it is worth noting

that the lower renal uptake of [^{68}Ga]Ga-P16-093 may contribute to the diagnosis of another urologic tumor, clear cell renal cell carcinoma (ccRCC), as the endothelial cells of the tumor-associated neovasculature of ccRCC express high levels of PSMA [29]. We have confirmed [^{68}Ga]Ga-P16-093 PET/CT demonstrates significantly better tumor detectability than 2- ^{18}F]FDG PET/CT for ccRCC patients [30]. By taking full advantage of the low urinary activity of [^{68}Ga]Ga-P16-093, it may be possible to expand the scope of application of this radiotracer and to identify genitourinary cancers more successfully than ever, which can result in better patient care and outcomes. However, [^{68}Ga]Ga-P16-093 exhibited a higher liver and spleen background than [^{68}Ga]Ga-PSMA-11 due to the stronger lipophilicity of the former. As concluded previously, high liver uptake could be a less significant interference factor for the diagnosis of PCa with [^{68}Ga]Ga-P16-093 PET/CT, because it is uncommon to have liver metastasis in these patients, especially in newly diagnosed primary PCa patients [14].

There are some limitations to our study. The most notable issue is the lack of surgical pathological confirmation of some PET-positive tumors. Most of patients did not complete their established operation plans in our hospital due to COVID-19 related travel restrictions. It was very difficult to obtain all tissue samples for histopathology due to ethical and practical constraints. However, all patients have a positive needle biopsy confirming the presence of PCa. A series of studies have previously documented the high accuracy of PSMA-11 PET for PSMA-avid lesions [23, 31]. Hence, given the consideration of the known limitations and pitfalls of PSMA PET, the interpretations of the tumors presented in this study remain credible. Another limitation is that we chose the noncancerous prostate tissue of patients rather than enrolling participants with benign prostate diseases (prostatic hyperplasia or prostatitis) to verify the cutoff SUVmax of the two radiotracers in detecting primary tumors. These results need to be further confirmed in subsequent studies.

Conclusion

In this prospective head-to-head study, [^{68}Ga]Ga-P16-093 PET/CT demonstrated significantly higher tumor uptake and detection capability than [^{68}Ga]Ga-PSMA-11 PET/CT, especially for intraprostatic lesions in low- and intermediate-risk PCa patients. Our findings suggest that [^{68}Ga]Ga-P16-093 is a novel radiotracer that may serve as an improved alternative to the routinely used [^{68}Ga]Ga-PSMA-11 in initial diagnosis and staging of primary PCa patients. These results warrant further investigation in a larger number of cohorts.

Funding This study was supported by the National High Level Hospital Clinical Research Funding (2022-PUMCH-C-004), the Fundamental Research Funds for the Central Universities (3332022110), Chinese Academy of Medical Science Innovation Fund for Medical Sciences (2022-I2M-C&T-A-008, 2022-I2M-2-002, 2021-I2M-1-016), Beijing Natural Science Foundation (M22035) and the National Natural Science Foundation of China (82272046).

Data availability Not applicable.

Declarations

Institutional review board statement Ethical approval was obtained from the Institute Review Board of Peking Union Medical College Hospital, Chinese Academy of Medical Sciences and Peking Union Medical College (no. ZS-2461), and this study was conducted in accordance with the principles of the Declaration of Helsinki.

Consent to participate Informed consent was obtained from all participants included in the study.

Conflicts of interest Hank F. Kung is the founder of Five Eleven Pharma, which holds the patent rights for [^{68}Ga]Ga-P16-093 and related technology. Other authors have no conflicts of interest or relevant financial activities to disclose.

References

1. Ghosh A, Heston WD. Tumor target prostate specific membrane antigen (PSMA) and its regulation in prostate cancer. *J Cell Biochem.* 2004;91:528–39. <https://doi.org/10.1002/jcb.10661>.
2. Masters SC, Hofling AA, Gorovets A, Marzella L. FDA approves Ga 68 PSMA-11 for prostate cancer imaging. *Int J Radiat Oncol Biol Phys.* 2021;111:27–8. <https://doi.org/10.1016/j.ijrobp.2021.03.055>.
3. Hofling AA, Fotenos AF, Niu G, Fallah J, Agrawal S, Wang SJ, et al. Prostate cancer theranostics: concurrent approvals by the Food and Drug Administration of the first diagnostic imaging drug indicated to select patients for a paired radioligand therapeutic drug. *J Nucl Med.* 2022;63:1642–3. <https://doi.org/10.2967/jnumed.122.264299>.
4. Hofman MS, Lawrentschuk N, Francis RJ, Tang C, Vela I, Thomas P, et al. Prostate-specific membrane antigen PET-CT in patients with high-risk prostate cancer before curative-intent surgery or radiotherapy (proPSMA): a prospective, randomised, multicentre study. *Lancet.* 2020;395:1208–16. [https://doi.org/10.1016/S0140-6736\(20\)30314-7](https://doi.org/10.1016/S0140-6736(20)30314-7).
5. Perera M, Papa N, Christidis D, Wetherell D, Hofman MS, Murphy DG, et al. Sensitivity, specificity, and predictors of positive ^{68}Ga -prostate-specific membrane antigen positron emission tomography in advanced prostate cancer: a systematic review and meta-analysis. *Eur Urol.* 2016;70:926–37. <https://doi.org/10.1016/j.eururo.2016.06.021>.
6. Schmuck S, von Klot CA, Henkenberens C, Sohns JM, Christiansen H, Wester HJ, et al. Initial experience with volumetric ^{68}Ga -PSMA I&T PET/CT for assessment of whole-body tumor burden as a quantitative imaging biomarker in patients with prostate cancer. *J Nucl Med.* 2017;58:1962–8. <https://doi.org/10.2967/jnumed.117.193581>.
7. Pattison DA, Debowski M, Gulhane B, Arnfield EG, Pelecanos AM, Garcia PL, et al. Prospective intra-individual blinded comparison of ^{18}F]PSMA-1007 and [^{68}Ga]Ga-PSMA-11 PET/CT imaging in patients with confirmed prostate cancer. *Eur J Nucl*

- Med Mol Imaging. 2022;49:763–76. <https://doi.org/10.1007/s00259-021-05520-y>.
8. Freitag MT, Radtke JP, Afshar-Oromieh A, Roethke MC, Hadaschik BA, Gleave M, et al. Local recurrence of prostate cancer after radical prostatectomy is at risk to be missed in ^{68}Ga -PSMA-11-PET of PET/CT and PET/MRI: comparison with mpMRI integrated in simultaneous PET/MRI. *Eur J Nucl Med Mol Imaging*. 2017;44:776–87. <https://doi.org/10.1007/s00259-016-3594-z>.
 9. Noto B, Buther F, Auf der Springe K, Avramovic N, Heindel W, Schafers M, et al. Impact of PET acquisition durations on image quality and lesion detectability in whole-body ^{68}Ga -PSMA PET-MRI. *EJNMMI Res*. 2017;7:12. <https://doi.org/10.1186/s13550-017-0261-8>.
 10. Lee H, Scheuermann JS, Young AJ, Doot RK, Daube-Witherspoon ME, Schubert EK, et al. Preliminary evaluation of ^{68}Ga -P16-093, a PET radiotracer targeting prostate-specific membrane antigen in prostate cancer. *Mol Imaging Biol*. 2022;24:710–20. <https://doi.org/10.1007/s11307-022-01720-6>.
 11. Zha Z, Ploessl K, Choi SR, Wu Z, Zhu L, Kung HF. Synthesis and evaluation of a novel urea-based ^{68}Ga -complex for imaging PSMA binding in tumor. *Nucl Med Biol*. 2018;59:36–47. <https://doi.org/10.1016/j.nucmedbio.2017.12.007>.
 12. Green MA, Hutchins GD, Bahler CD, Tann M, Mathias CJ, Territo W, et al. [^{68}Ga]Ga-P16-093 as a PSMA-targeted PET radiopharmaceutical for detection of cancer: initial evaluation and comparison with [^{68}Ga]Ga-PSMA-11 in prostate cancer patients presenting with biochemical recurrence. *Mol Imaging Biol*. 2020;22:752–63. <https://doi.org/10.1007/s11307-019-01421-7>.
 13. Bahler CD, Green MA, Tann MA, Swensson JK, Collins K, Alexoff D, et al. Assessing extra-prostatic extension for surgical guidance in prostate cancer: comparing two PSMA-PET tracers with the standard-of-care. *Urol Oncol*. 2023;41(48):e1–9. <https://doi.org/10.1016/j.urolonc.2022.10.003>.
 14. Wang G, Hong H, Zang J, Liu Q, Jiang Y, Fan X, et al. Head-to-head comparison of [^{68}Ga]Ga-P16-093 and [^{68}Ga]Ga-PSMA-617 in dynamic PET/CT evaluation of the same group of recurrent prostate cancer patients. *Eur J Nucl Med Mol Imaging*. 2022;49:1052–62. <https://doi.org/10.1007/s00259-021-05539-1>.
 15. Wang G, Li L, Zang J, Hong H, Zhu L, Kung HF, et al. Head-to-head comparison of ^{68}Ga -P16-093 and ^{68}Ga -PSMA-617 PET/CT in patients with primary prostate cancer: a pilot study. *Clin Nucl Med*. 2023;48:289–95. <https://doi.org/10.1097/RLU.00000000000004566>.
 16. Mohler JL, Antonarakis ES, Armstrong AJ, D'Amico AV, Davis BJ, Dorff T, et al. Prostate cancer, version 2.2019, NCCN clinical practice guidelines in oncology. *J Natl Compr Canc Netw*. 2019;17:479–505. <https://doi.org/10.6004/jnccn.2019.0023>.
 17. Fendler WP, Eiber M, Beheshti M, Bomanji J, Ceci F, Cho S, et al. ^{68}Ga -PSMA PET/CT: joint EANM and SNMMI procedure guideline for prostate cancer imaging: version 1.0. *Eur J Nucl Med Mol Imaging*. 2017;44:1014–24. <https://doi.org/10.1007/s00259-017-3670-z>.
 18. Suh M, Im HJ, Ryoo HG, Kang KW, Jeong JM, Prakash S, et al. Head-to-head comparison of ^{68}Ga -NOTA (^{68}Ga -NGUL) and ^{68}Ga -PSMA-11 in patients with metastatic prostate cancer: a prospective study. *J Nucl Med*. 2021;62:1457–60. <https://doi.org/10.2967/jnumed.120.258434>.
 19. Sonni I, Eiber M, Fendler WP, Alano RM, Vangala SS, Kishan AU, et al. Impact of ^{68}Ga -PSMA-11 PET/CT on staging and management of prostate cancer patients in various clinical settings: a prospective single-center study. *J Nucl Med*. 2020;61:1153–60. <https://doi.org/10.2967/jnumed.119.237602>.
 20. Uprimny C, Kroiss AS, Decristoforo C, Fritz J, von Guggenberg E, Kendler D, et al. ^{68}Ga -PSMA-11 PET/CT in primary staging of prostate cancer: PSA and Gleason score predict the intensity of tracer accumulation in the primary tumour. *Eur J Nucl Med Mol Imaging*. 2017;44:941–9. <https://doi.org/10.1007/s00259-017-3631-6>.
 21. Woythal N, Arsenic R, Kempkensteffen C, Miller K, Janssen JC, Huang K, et al. Immunohistochemical validation of PSMA expression measured by ^{68}Ga -PSMA PET/CT in primary prostate cancer. *J Nucl Med*. 2018;59:238–43. <https://doi.org/10.2967/jnumed.117.195172>.
 22. Kaemmerer D, Peter L, Lupp A, Schulz S, Sanger J, Prasad V, et al. Molecular imaging with ^{68}Ga -SSTR PET/CT and correlation to immunohistochemistry of somatostatin receptors in neuroendocrine tumours. *Eur J Nucl Med Mol Imaging*. 2011;38:1659–68. <https://doi.org/10.1007/s00259-011-1846-5>.
 23. Fendler WP, Calais J, Eiber M, Flavell RR, Mishoe A, Feng FY, et al. Assessment of ^{68}Ga -PSMA-11 PET accuracy in localizing recurrent prostate cancer: a prospective single-arm clinical trial. *JAMA Oncol*. 2019;5:856–63. <https://doi.org/10.1001/jamaoncol.2019.0096>.
 24. Park SY, Zacharias C, Harrison C, Fan RE, Kunder C, Hatami N, et al. Gallium 68 PSMA-11 PET/MR imaging in patients with intermediate- or high-risk prostate cancer. *Radiology*. 2018;288:495–505. <https://doi.org/10.1148/radiol.2018172232>.
 25. Zhou C, Tang Y, Deng Z, Yang J, Zhou M, Wang L, et al. Comparison of ^{68}Ga -PSMA PET/CT and multiparametric MRI for the detection of low- and intermediate-risk prostate cancer. *EJNMMI Res*. 2022;12:10. <https://doi.org/10.1186/s13550-022-00881-3>.
 26. Cytawa W, Seitz AK, Kircher S, Fukushima K, Tran-Gia J, Schirbel A, et al. ^{68}Ga -PSMA I&T PET/CT for primary staging of prostate cancer. *Eur J Nucl Med Mol Imaging*. 2020;47:168–77. <https://doi.org/10.1007/s00259-019-04524-z>.
 27. Klingenberg S, Jochumsen MR, Ulhoi BP, Fredsoe J, Sorensen KD, Borre M, et al. ^{68}Ga -PSMA PET/CT for primary lymph node and distant metastasis NM staging of high-risk prostate cancer. *J Nucl Med*. 2021;62:214–20. <https://doi.org/10.2967/jnumed.120.245605>.
 28. Kuten J, Fahoum I, Savin Z, Shamni O, Gitstein G, Hershkowitz D, et al. Head-to-head comparison of ^{68}Ga -PSMA-11 with ^{18}F -PSMA-1007 PET/CT in staging prostate cancer using histopathology and immunohistochemical analysis as a reference standard. *J Nucl Med*. 2020;61:527–32. <https://doi.org/10.2967/jnumed.119.234187>.
 29. Chang SS, Reuter VE, Heston WD, Bander NH, Grauer LS, Gaudin PB. Five different anti-prostate-specific membrane antigen (PSMA) antibodies confirm PSMA expression in tumor-associated neovasculature. *Cancer Res*. 1999;59:3192–8.
 30. Wang G, Li L, Wang J, Zang J, Chen J, Xiao Y, et al. Head-to-head comparison of [^{68}Ga]Ga-P16-093 and 2- ^{18}F]FDG PET/CT in patients with clear cell renal cell carcinoma: a pilot study. *Eur J Nucl Med Mol Imaging*. 2023;50:1499–509. <https://doi.org/10.1007/s00259-022-06101-3>.
 31. Caroli P, Sandler I, Matteucci F, De Giorgi U, Uccelli L, Celli M, et al. ^{68}Ga -PSMA PET/CT in patients with recurrent prostate cancer after radical treatment: prospective results in 314 patients. *Eur J Nucl Med Mol Imaging*. 2018;45:2035–44. <https://doi.org/10.1007/s00259-018-4067-3>.

Publisher's note Springer Nature remains neutral with regard to jurisdictional claims in published maps and institutional affiliations.

Springer Nature or its licensor (e.g. a society or other partner) holds exclusive rights to this article under a publishing agreement with the author(s) or other rightsholder(s); author self-archiving of the accepted manuscript version of this article is solely governed by the terms of such publishing agreement and applicable law.

Authors and Affiliations

Guochang Wang¹ · Linlin Li¹ · Ming Zhu² · Jie Zang³ · Jiarou Wang¹ · Rongxi Wang¹ · Weigang Yan² · Lin Zhu⁴ · Hank F. Kung⁵ · Zhaohui Zhu¹

✉ Weigang Yan
ywgpumch@sina.com

✉ Lin Zhu
zhulin@bnu.edu.cn

✉ Hank F. Kung
kunghf@sunmac.spect.upenn.edu

✉ Zhaohui Zhu
13611093752@163.com

¹ Department of Nuclear Medicine, State Key Laboratory of Complex Severe and Rare Diseases, Beijing Key Laboratory of Molecular Targeted Diagnosis and Therapy in Nuclear Medicine, Peking Union Medical College Hospital, Chinese Academy of Medical Sciences, Peking Union Medical College, Beijing 100730, China

² Department of Urology, Peking Union Medical College Hospital, Chinese Academy of Medical Sciences, Peking Union Medical College, Beijing 100730, China

³ Department of Nuclear Medicine, The First Affiliated Hospital of Fujian Medical University, Fuzhou 350005, China

⁴ College of Chemistry, Key Laboratory of Radiopharmaceuticals, Ministry of Education, Beijing Normal University, Beijing 100875, China

⁵ Department of Radiology, University of Pennsylvania, Philadelphia, PA 19104, USA